



**INSTITUTO  
DA ÁGUA**

## **Qualidade da Água em Estuários Portugueses Water Quality in Portuguese Estuaries**



### **Estuário do Mira**

**Directiva do Tratamento de Águas Residuais Urbanas**

**(91/271/CEE)**

**Directiva dos Nitratos de Origem Agrícola**

**(91/676/CEE)**



**2002**

## ABSTRACT

This report describes a numerical study of trophic processes in Mira Estuary (Portugal), aiming to identify and evaluate the factors that determine the trophic level of the estuary. The study includes (i) a description of the hydrodynamics of the estuary, its residence time and the interaction between different regions of the estuary, (ii) a simulation of trophic processes in present conditions and (iii) forecast of the implications of a nutrients load increase.

The study shows that phytoplankton is both bottom-up controlled by low availability of nutrients and top-down controlled by secondary producers. The estuary imports nutrients from the sea, which are transported to the middle estuary by diffusion generated by tidal oscillation and exports phytoplankton, organic matter and zooplankton. Residence time is in the order of two weeks, being in the order of days in the lower estuary.

Concentration of phytoplankton is more than 95% of the time, below  $5\mu\text{g Chl a/L}$  showing that the trophic level of the estuary can be classified as low, as it was classified by IMAR, which as collected historical field data and applied the NEEA-NOAA index for classifying the trophic level of the estuary.

A scenario of doubling the nutrients load was also simulated. In this scenario, the bottom-up limiting factor of phytoplankton was reduced, the carrying capacity of secondary producers was increased, but the estuary would still import nutrients from the sea. The maintenance of phytoplankton biomass and the increase of zooplankton biomass is a result of top-down control of phytoplankton concentration.

# INDEX

<b>ABSTRACT</b>	<b>2</b>
<b>1 INTRODUCTION</b>	<b>7</b>
<b>2 MIRA ESTUARY</b>	<b>9</b>
2.1 Estuary loads	10
<b>3 HYDRODYNAMIC MODEL</b>	<b>13</b>
3.1 Model Grid	13
3.2 Transient Circulation	15
3.3 Residual Circulation	16
3.4 Residence Time	17
3.5 Interaction between parts of the estuary	21
<b>4 ECOLOGICAL MODEL</b>	<b>23</b>
4.1 Reference situation	23
4.1.1 Time Series Analysis (Field Data and Model Results)	24
4.1.2 Spatial Distributions of Concentration	27
4.1.3 Annual Average Distributions of Properties per Zone of the Estuary	30
4.1.3.1 Annual Budgets per Zone of the Estuary	33
4.1.3.2 Conclusion of reference situation	33
4.1.4 Scenario of Nitrate Discharge Increasing	35
4.1.4.1 Spatial Distributions	36
4.1.4.2 Annual Distribution	36
4.1.4.3 Annual Budgets per Zone of the Estuary	39
<b>5 CONCLUSIONS</b>	<b>41</b>
<b>ANNEX - WASTE WATER TREATMENT PLANTS</b>	<b>43</b>

## FIGURES INDEX

FIGURE 1: MIRA ESTUARY AND STUDY AREA CONSIDERED IN THIS WORK (ZONE 1 AND ZONE 2), (ADAPTED FROM SILVA DE ALMEIDA, 2000).	9
FIGURE 2: LOCATION OF FIELD STATION PT.EN.120 AND ALB. STA. CLARA.	11
FIGURE 3: AVERAGE MONTHLY DISTRIBUTIONS OF SOME PROPERTIES OF MIRA RIVER.	11
FIGURE 4: NUTRIENTS CONCENTRATIONS VS MIRA RIVER FLOW RATE.	12
FIGURE 5: BATHYMETRY OF THE MIRA ESTUARY USED BY THE MODEL. THE UPPER PART OF THE ESTUARY WAS RECTIFIED AND ALIGNED WITH THE GEOGRAPHICAL AXIS FOR COMPUTATIONAL EFFICIENCY.	14
FIGURE 6 : GRID OF 20X20 METERS USED IN THE LOWER ESTUARY, WHERE DETAILED BATHYMETRIC INFORMATION IS AVAILABLE.	15
FIGURE 7: VELOCITY FIELD DURING A SPRING TIDE FOR EBB (LEFT) AND FLOOD (RIGHT) CONDITIONS.	15
FIGURE 8: VELOCITY FIELD DURING A NEAP TIDE FOR EBB (LEFT) AND FLOOD (RIGHT) CONDITIONS.	16
FIGURE 9: RESIDUAL SPECIFIC FLUX IN THE MOUTH OF MIRA ESTUARY.	17
FIGURE 10: INITIAL DISTRIBUTION OF THE LAGRANGIAN TRACERS IN THE MIRA ESTUARY.	18
FIGURE 11: EVOLUTION OF THE WATER VOLUME INSIDE THE MIRA ESTUARY DURING A SPRING-NEAP CYCLE.	19
FIGURE 12: DISTRIBUTION OF THE LAGRANGIAN TRACERS IN THE MIRA ESTUARY AFTER 7 DAYS (NO WIND).	20
FIGURE 13: DISTRIBUTION OF THE LAGRANGIAN TRACERS IN THE MIRA ESTUARY AFTER 15 DAYS (NO WIND).	20
FIGURE 14: EVOLUTION OF THE RATIO BETWEEN THE VOLUME OF LAGRANGIAN TRACERS INSIDE THE ESTUARY AND THE TOTAL ESTUARY VOLUME AS A FUNCTION OF THE TIME (NO WIND).	21
FIGURE 15: WATER EXCHANGES AMONG BOXES (RESULTS INTEGRATED PERIOD FOR 7 DAYS).	22
FIGURE 16: WATER EXCHANGES AMONG BOXES (RESULTS INTEGRATED PERIOD FOR 15 DAYS).	22
FIGURE 17: LOCATION OF FIELD STATIONS OF IPIMAR'S CAMPAIGNS AND CORRESPONDENT BOX FOR EACH STATION IN MIRA ESTUARY.	25
FIGURE 18: TIME SERIES OF MODEL RESULTS (BLUE POINTS) FOR WHOLE ESTUARY AND PHYTOPLANKTON FIELD DATA FOR 1989 (IPIMAR) IN THE REFERENCE SITUATION.	25
FIGURE 19: ANNUAL AVERAGE CONCENTRATIONS COMPUTED BY MODEL AND MEASURED IN BOXES FOR REFERENCE SITUATION.	26
FIGURE 20: TIME SERIES OF MODEL RESULTS IN STATION#1 FOR REFERENCE SITUATION.	28
FIGURE 21: TIME SERIES OF MODEL RESULTS IN STATION#3 FOR REFERENCE SITUATION.	28
FIGURE 22: TIME SERIES OF MODEL RESULTS IN STATION#5 FOR REFERENCE SITUATION.	29
FIGURE 23: TIME SERIES OF MODEL RESULTS IN STATION#7 FOR REFERENCE SITUATION.	29
FIGURE 24: TIME SERIES OF MODEL RESULTS IN STATION#9 FOR REFERENCE SITUATION.	30
FIGURE 25: SPATIAL DISTRIBUTION OF PHYTOPLANKTON, AMMONIA, NITRATE AND OXYGEN IN THE REFERENCE SITUATION DURING EBB (LEFT) AND FLOOD (RIGHT).	31
FIGURE 26: ANNUAL AVERAGE VALUES OF PHYTOPLANKTON, OM, NITRATE AND AMMONIA PER BOX IN THE ESTUARY FOR THE REFERENCE SITUATION.	32
FIGURE 27: CUMULATIVE FREQUENCY FOR PHYTOPLANKTON IN SEAWATER, MIXING AND FRESHWATER ZONES.	32
FIGURE 28: ANNUAL MASS FLUXES BETWEEN ZONES OF ESTUARY.	34
FIGURE 29: ANNUAL BUDGETS BETWEEN BOXES IN THE REFERENCE SITUATION.	35

FIGURE 30: TOTAL BALANCE IN MIRA ESTUARY FOR THE REFERENCE SITUATION.	35
FIGURE 31: COMPARISON OF CONCENTRATIONS FOR REFERENCE SITUATION (LEFT) WITH A SCENARIO OF NITRATE LOAD DOUBLING (RIGHT) (WINTER, LOW WATER SCENARIO).	37
FIGURE 32: AVERAGE ANNUAL CONCENTRATION IN REFERENCE SITUATION AND IN THE SCENARIO OF DOUBLING NITRATE RIVER LOAD.	38
FIGURE 33: OXYGEN CONSUMPTION FOR OXIDATION OF ORGANIC MATER IN REFERENCE SITUATION AND IN THE SCENARIO OF DOUBLING NITRATE RIVER LOAD	39
FIGURE 34: ANNUAL BUDGETS IN THE REFERENCE SITUATION AND IN THE SCENARIO OF DOUBLING NITRATE RIVER LOAD.	40
FIGURE 35: TOTAL BALANCE OF ESTUARY IN THE REFERENCE SITUATION AND IN THE SCENARIO OF DOUBLING NITRATE RIVER LOAD.	40

## TABLES INDEX

TABLE 1: TYPICAL MIRA RIVER WATER PROPERTIES (STATION PT.EN.120, IN FIGURE 2)..	12
TABLE 2: SAMPLING PERIODS IN THE MIRA ESTUARY.....	24
TABLE 3: ODEMIRA AND V. N. DE MILFONTES WASTE WATER TREATMENT PLANT CHARACTERISTICS. ....	43
TABLE 4: LOADS ESTIMATED BEFORE AND AFTER EACH TREATMENT PLANT.....	43
TABLE 5: TYPICAL VALUES OF LOADS PER INHABITANT PER DAY (SARAIVA, 2001).....	44
TABLE 6: REMOVAL EFFICIENCY OF WWTP CONSIDERED WHEN NO MEASURED DATA WAS AVAILABLE (SARAIVA, 2001).....	44

## 1 INTRODUCTION

An estuary is a coastal transitional water body where fresh water mixes with marine water. Trophic processes occurring in estuaries depend essentially on nutrient loads and on their physical properties, where residence time plays a major role. Another major physical factor controlling biological activity is turbidity, which reduces light penetration and depends on the mean depth, wind fetch and sediment distribution in the estuary. This study was preceded by similar studies for the Tagus, Sado and Mondego estuaries. Which has put into evidence different types of control of trophic level by physical processes.

In Tagus estuary, the trophic level is limited by light penetration, which is controlled by high concentration of suspended matter. In this estuary the tidal flats extend for about 100 km<sup>2</sup> and the wind fetch can be longer than 20 km. As a consequence typical wind waves are higher than 0.2 m enhancing resuspension by tidal currents. Residence time is of the order of 3 weeks, and primary production is not limited by nutrients.

In Sado estuary primary production is bottom-up limited by nutrients and top-down limited by zooplankton. Residence time is of the order of 2 months giving time enough for particulate organic matter to settle and remineralize at the bottom. As a consequence the concentration of phytoplankton in the estuary remains low (typically below 5 µg Chl a /L) and displays the oscillatory character typical from “prey-predator” relation.

In Mondego estuary primary production is limited by residence time, which is less than 4 days. Nutrient load is very high, but phytoplankton has no time to develop a bloom before leaving the estuary. In these conditions only the benthic macro-algae has the possibility to grow in the estuary.

Trophic activity in Mira estuary is bottom-up limited by nutrients and top-down limited by zooplankton, as in Sado estuary. The oscillatory character displayed by the Sado estuary is not found in Mira estuary, because residence time and settling areas in the Mira are not large enough to make possible mineralization of organic matter inside the estuary. Another important process for biological activity in the Mira, is the strong mixing of estuarine and sea water at the lower estuary.

Due to the physical features of Mira estuary and because nutrient loads carried by the river are very small, primary production is small and phytoplankton concentration is, more than 95% of the time, below 5  $\mu\text{g Chl a /L}$ . The estuary imports nitrate from the ocean and exports phytoplankton, organic matter and zooplankton.

This study was carried out using an integrated hydro-ecological model MOHID (<http://www.mohid.com>) developed at Maretec, a Research Centre of Instituto Superior Técnico, and complements another study carried out by IMAR, which as collected historical field data and applied the NEEA-NOAA index for classifying the trophic level of the estuary. According to that index the trophic level of the estuary should be classified as *low*. The application of the same index to the results of the model has generated the same classification.

After the model results validation for the reference situation, a scenario of doubling nutrient loads was simulated. Results show that even for those conditions the trophic level would be *low* and the estuary would still import nutrients from the ocean. Concentration of phytoplankton would still be top limited and the main consequence of a higher availability of nutrients would be an increase in the concentration of zooplankton.



## 2 MIRA ESTUARY

Mira river basin is located in the Southwest coast of Portugal. The river rises in Caldeirão Mountain – about 470 m high - and flows Northward along about 145 Km long, to reach the estuary off Vila Nova de Milfontes, 30 Km Southward of Sines.

Mira estuary, represented in Figure 1, is a long (32 km) and narrow estuary (maximum width of 150 m). The average depth of the estuary is 6 m and its maximum depth, 16 m, is reached near the mouth. The estuary is oriented along the Northwest-Southeast direction, conferring it a favourable exposure to predominant northwest coastal winds, which generate surface waves and enhance vertical mixing. Discharge of the river into the estuary is controlled by Santa Clara reservoir, located ahead of Odemira, the main population aggregate in the upper estuary.



**Figure 1: Mira estuary and study area considered in this work (Zone 1 and Zone 2), (Adapted from Silva de Almeida, 2000).**

The lower estuary - zone 1 in Figure 1 - has clear marine properties and the upper estuary - zone 3 in the figure – is mostly fresh water. Major gradients are located in

zone 2 where mixing of marine and fresh water occurs, mostly due to tidal oscillation. Small salt marshes can be found on the banks located along marine and brackish zones, which stimulate longitudinal shear diffusion in the estuary. The upper zone is quite narrow and shallow and has a small contribution for the tidal prism of the estuary, which is demonstrated by the results of the hydrodynamic model. The velocities computed by the model close to the mouth of the estuary are identical to the velocities measured (not represented), showing that the tidal prism computed and simulated is similar.

## 2.1 ESTUARY LOADS

Nutrient loads were grouped into (i) river nutrients (Mira) and (ii) discharges from Urban Waste Water Treatment Plants (UWWTP). Loads are characterized in terms of discharge and concentrations of Nitrate, Ammonia ( $\text{NH}_4^+$ ), Nitrite and Organic Matter. Nutrients may reach the estuary through diffuse loads as lixiviation of agricultural land or through punctual loads as UWWTP.

Figure 2 shows the drainage basin of Mira estuary. In this figure it can be seen Santa Clara reservoir in the upper river and two monitoring stations, run by INAG<sup>1</sup>. Santa Clara reservoir is a major feature at the basin, which strongly modulates river discharge. Discharges have been measured at the downstream station, off Odemira, and water properties have been measured in both stations.

Figure 3 shows monthly values measured in the downstream station and Table 1 shows the values considered for discharge. Water discharge varies between a nil value during the dry season, and 12. m<sup>3</sup>/s during the raining season in winter. Average discharge is 2.9 m<sup>3</sup>/s and the modal discharge is 0.5 m<sup>3</sup>/s. Concentrations of ammonia and nitrate in the river are quite small. Nitrate shows a tendency for increasing with river discharge, while ammonia is quite constant (Figure 4). Concentration of suspended solids is also quite low and uniform.

---

<sup>1</sup> Data collected in the monitoring stations run by INAG-Instituto da Água is published at <http://snirh.inag.pt/snirh/>



Figure 2: Location of Field Station PT.EN.120 and Alb. Sta. Clara.

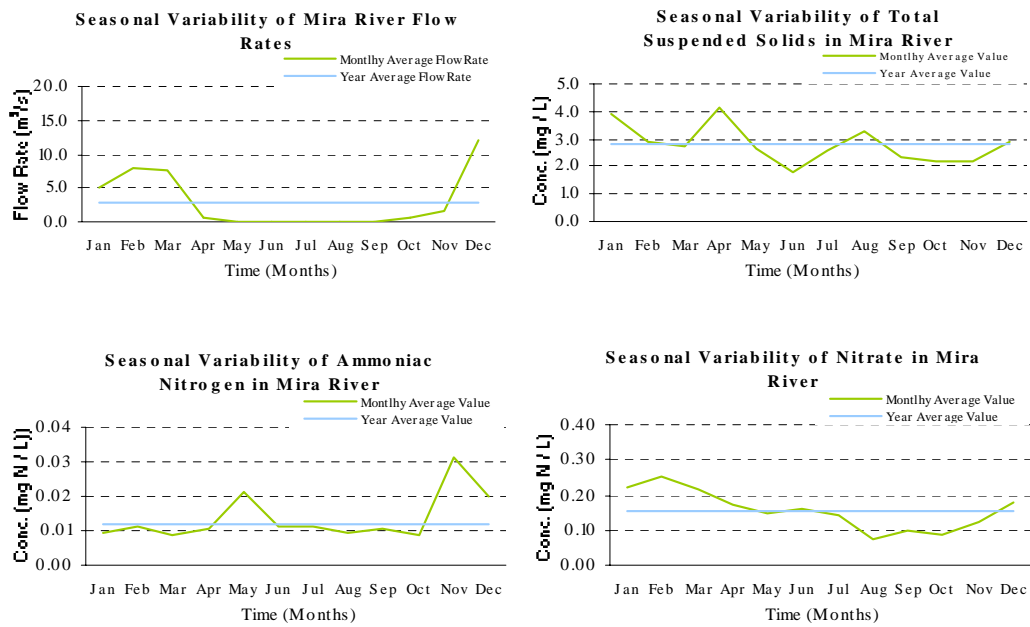
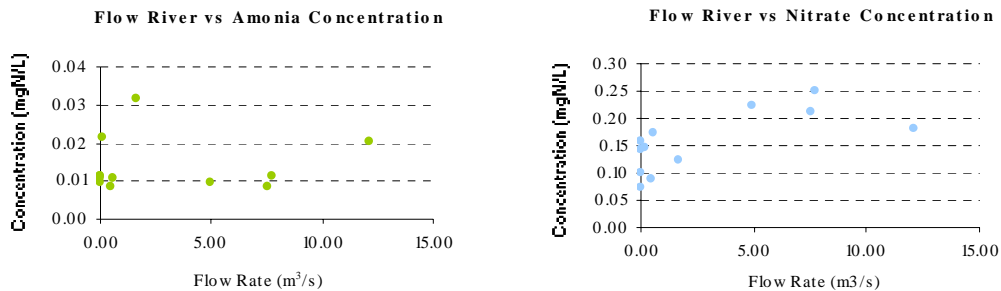


Figure 3: Average monthly distributions of some properties of Mira River.

**Table 1: Typical Mira River water properties (Station PT.EN.120, in Figure 2)**

Name	Units	Value
Flow	m <sup>3</sup> / s	0.5
Nitrate	mg N / L	0.16
Nitrite	mg N / L	0.005
Dissolved Oxygen	mg O <sub>2</sub> / L	8.3
Biological Oxygen demand	mg O <sub>2</sub> / L	2.2
Total Solids	mg / L	4.15
Ammonia	mg N / L	0.012
Dissolved Organic Nitrogen Refractory	mg N / L	0
Dissolved Organic Nitrogen Non Refractory	mg N / L	0.2
Particulate Organic Nitrogen	mg N / L	0.2
Phytoplankton	mg C/L	0.15
Zooplankton	mg C / L	0.015



**Figure 4: Nutrients concentrations vs Mira River flow rate.**

Odemira and Vila Nova de Milfontes are small agglomerations located respectively upstream of the estuary and at its mouth. Characteristics of the respective WWTP are given in ANNEX 1. Discharge of Odemira WWTP (0.003 m<sup>3</sup>/s) is included at the river load and discharge of Milfontes WWTP(0.007 m<sup>3</sup>/s) is disposed directly in the sea.

### 3 Hydrodynamic Model

Hydrodynamics provides basic information to study biogeochemical processes in marine systems. It determines vertical mixing, transport and consequently residence time in the estuary, which determine the fate of nutrients and organic matter discharged by the river in the upper estuary or, by the smaller tributaries or by anthropogenic discharges in the lower reaches.

Hydrodynamic circulation in the estuary is forced by tide and river discharge. Wind forcing generates vertical mixing, but can't modify the flow because the estuary is too narrow to allow the generation of horizontal eddies by wind shear. Tidal levels used in the present study were measured in Sines tidal gauge, 30 km northward. River discharge used for this study ( $0.5 \text{ m}^3 \text{ s}^{-1}$ ) is the most frequent value of a four years series 1958, 59, 60 e 61).

Residence time in the estuary and tidal circulation are described for a spring-neap tide cycle. Long-term water quality simulations were performed for average tidal conditions for computational reasons. Average tidal conditions represented by the M2 tidal component were simulated and stored into a file and were read cyclically for long runs.

#### 3.1 MODEL GRID

The detail of the grid to use in a model must be adequate for the purpose of the model and consistent with the detail of the data available. For hydrodynamics simulations, the most detailed grid provides, generates the best results. For water quality simulations a coarser grid is adequate because concentration gradients are smaller than velocity gradients.

In case of Mira estuary there is a very detailed bathymetry for the lower (and wider) 4 km of the estuary and a set of cross sections along the next 16 km (about the lower limit of zone 3 in Figure 1). Upstream of that region there is no bathymetric information because the contribution of the tidal prism in that area is not relevant for the hydrodynamics of the estuary.

To study the hydrodynamics of the estuary a grid of 20\*20 metres is used at the lower and wider part of the estuary. This grid is fine enough to individualise the channels in that part of the estuary and is consistent with the detail of the bathymetric information.

Upstream of that region the grid size increases to reach 200 meters in the upper part of the estuary.

In order to optimise computer resources required by the model (memory allocation), the estuary was rectified. This approach is consistent with the detail of the bathymetric information available and it is also consistent with the geometry of the estuary, which is mainly rectilinear. The approach validity is also demonstrated by the comparison of model results and field measurements. Figure 5 shows the bathymetry used for the hydrodynamic simulations and Figure 6 shows a zoom of the grid in the lower estuary where detailed bathymetric information is available. Black areas correspond to intertidal regions.

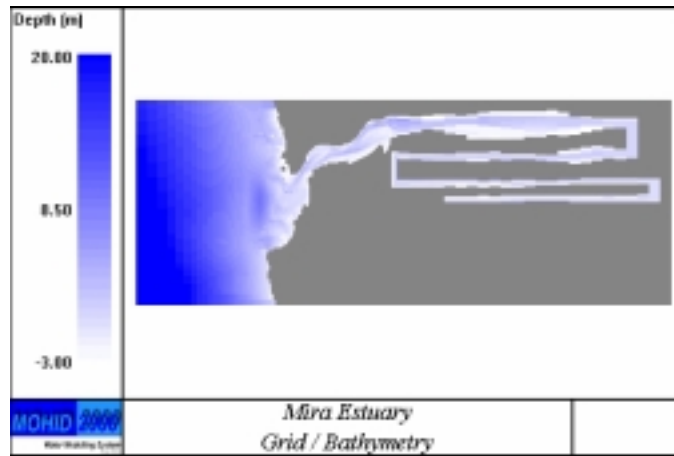


**Figure 5: Bathymetry of the Mira estuary used by the model. The upper part of the estuary was rectified and aligned with the geographical axis for computational efficiency.**

To study the ecological processes, this grid was integrated merging 2x2 grid cells into one, using an integration algorithm that grants transport consistency. This technique allows for a shorter computational time, without compromising the quality of the results (advective fluxes are computed precisely). Using this technique, the simulation of two years requires 4 computing days on an average computer (Pentium at 1.8 GHz).

The area of the estuary considered in the simulations is large enough to allow the consideration of uniform properties along the open boundary because it is far enough of the estuary mouth to consider properties independent of tidal situation.

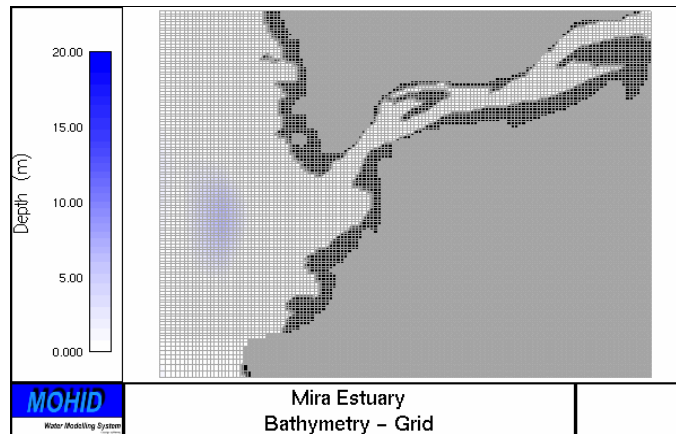


Figure 6 : Grid of 20x20 meters used in the lower estuary, where detailed bathymetric information is available.

### 3.2 TRANSIENT CIRCULATION

Transient circulation describes the instantaneous flow, which in case of the Mira is generated by tide and by river discharge. To describe transient circulation, the model run using the fine grid presented in Figure 6 and forced with all components and with the average discharge of Mira River ( $0.5 \text{ m}^3 \text{ s}^{-1}$ ). Simulations including both spring-neap tidal conditions were accomplished and results are shown below for flooding and ebb conditions. In all figures, colour represents velocity magnitude and arrows magnitude and direction. Scales are indicated on the left side of the figures.

Figure 7 and Figure 8 show the flow in the lower estuary during ebb (on the left) and flooding (on the right) in spring and neap conditions, respectively. These figures show that during ebb, the velocity is clearly higher than during flood and that the maximum velocity in spring tide exceeds 1 m/s at the mouth of the estuary.

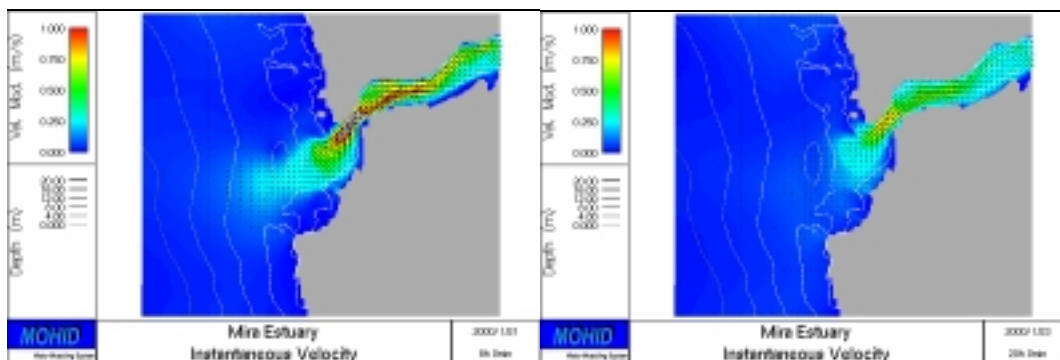


Figure 7: Velocity field during a spring tide for ebb (left) and flood (right) conditions.

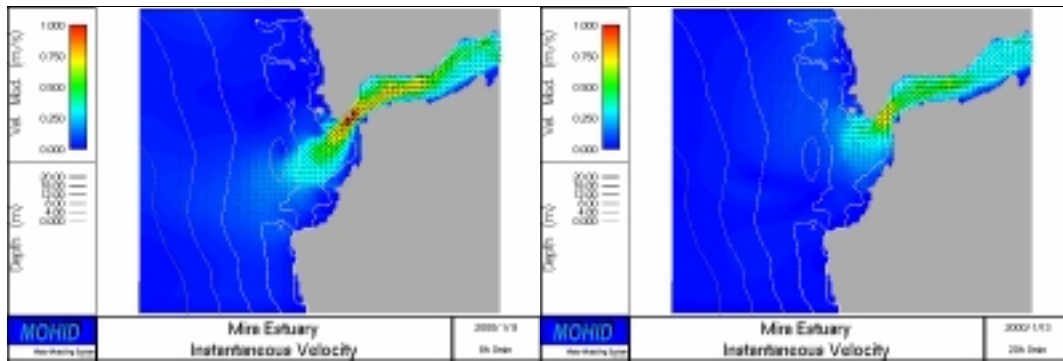


Figure 8: Velocity field during a neap tide for ebb (left) and flood (right) conditions.

### 3.3 RESIDUAL CIRCULATION

Residual circulation represents the local average of transient circulation, giving information about preferential transport in the estuary. Residual circulation can be defined in several ways: (i) as the average of transient velocity field (m/s), (ii) as average of transient water flux per unit of length –residual specific flux ( $\text{m}^2/\text{s}$ ) - or (iii) as residual specific flux divided by the local average depth of the water column – which is also a velocity - (m/s). Among the three results, only residual flux has null divergence.

Residual velocity at the estuary was computed integrating the flow over a period of 15 days, which is much longer than the time periods, associated to the variability of transient flow. Figure 9 shows residual velocity derived from residual flux in the lower estuary. This figure shows one large eddy near the estuary mouth adjacent to the ebb jet, with residual velocities of, 10 cm/s. This eddy shows that water leaving the estuary is projected far off the estuary mouth and has a tendency for recirculating northwards. The leg of this eddy close to the mouth moves southward, creating conditions for renewal of estuarine water along that side of the estuary. This dynamics minimizes the amount of ebb water re-entering the estuary, contributing for shortening residence time inside the estuary. Coastal currents induced by local wind and/or by regional circulation also contribute to remove ebb water from the region of the mouth reducing also residence time inside the estuary.



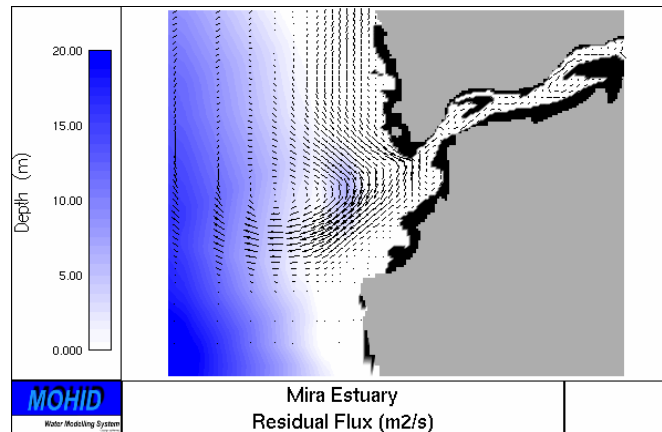


**Figure 9: Residual specific flux in the mouth of Mira Estuary.**

### **3.4 RESIDENCE TIME**

Residence time is an important indicator for understanding the ecological dynamics of estuaries. Estuaries with a short residence time will export nutrients from upstream sources more rapidly than estuaries with longer residence time. Three categories can be considered: (i) estuaries where residence time is shorter than time required to develop a bloom, (ii) estuaries where residence time is long enough to develop a bloom, but shorter than time required for mineralizing the products of that bloom and (iii) estuaries where residence time allow for mineralization of the products of the bloom, allowing for several picks of production during one year.

There are several ways for computing residence time, depending on the information available. A clear overview is given in the Technical Guidance Manual for Nutrient Criteria (EPA, 2001). The availability of a numerical model - as is the case in this study - allows for the most detailed calculation. Here, residence time is defined as the time required by water to leave the estuary and is computed using lagrangian tracers, which are used for labelling water and to monitor its location.

Different regions inside the estuary are identified by “boxes”, which are uniformly filled with tracers, representing each the same volume of water. Tracer’s locations are monitored, as well as their residence time inside each part of the estuary and time required for leaving the estuary.

Estuary residence time was computed performing the following steps:

- ✓ Computation of hydrodynamics forced by tide and by the most frequent river discharge ( $0.5 \text{ m}^3 \text{ s}^{-1}$ ),
- ✓ Division of the estuary into boxes and labelling of its water using lagrangian tracers. Total amount of tracers and their initial distribution in each box are calculated so that the total volume of tracers released inside each box matches its water volume,
- ✓ Calculation of residence time as shown in the appendix describing model details.

Figure 10 shows the initial distribution of lagrangian tracers in the estuary.

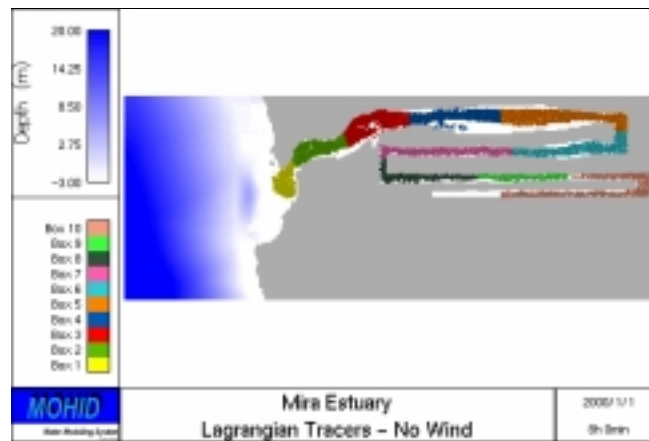


**Figure 10: Initial distribution of lagrangian tracers in the Mira estuary.**

The total volume of tracers in the estuary, at the beginning of simulation, is equal to the total volume of water inside the estuary at the releasing instant. Starting simulations at high water maximizes the number of tracers to use for labeling estuarine water, making the study more comprehensive.

Figure 11 shows water volume evolution inside the estuary during simulation period. This figure shows that the average volume of the estuary is about  $8.5 \times 10^6 \text{ m}^3$  and the average tidal prism (difference between the volume of the estuary in high water and low water), is about  $6 \times 10^6 \text{ m}^3$ , which represents about one half of the water inside the estuary in high water. Average daily discharge of the river is  $4.3 \times 10^4 \text{ m}^3$ , which is less than 1% of the tidal prism. The ratio between the two numbers suggests that mixing plays a major role on residence time in the estuary.

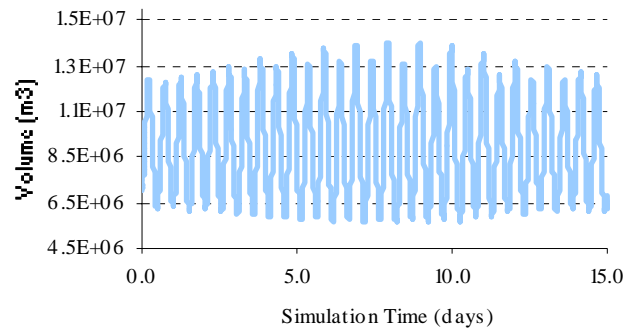


**Figure 11: Evolution of water volume inside the Mira estuary during a spring-neap cycle.**

To evaluate residence time inside Mira estuary the model was forced by all tidal harmonics and by the most frequent river discharge. Figure 12 and Figure 13 show the distribution of lagrangian tracers at low water respectively 7 and 15 days after tracer releasing and Figure 14 shows the evolution of the contribution of volume of tracer still in the estuary for the volume of the estuary in each instant of time.

In Figure 12 and in Figure 13, it is possible to observe that tracers are gradually flushed out off the estuary, which is consistent with the evolution shown in Figure 14. Most tracers leave the estuary southward, transported by the ebb jet and then turn northward as a consequence of the coriolis force, which turns the jet rightwards and generates the residual eddy at the mouth of the estuary as shown in Figure 9. Analysis of the distributions of tracers shows a clear zone at the upper estuary and another at the lower estuary<sup>2</sup>.

Clean zones are zones where the water has been replaced by new water. In the upper estuary new water is river fresh water, and close to the mouth, new water is marine water. The analysis of figure 14 shows that fresh water from the river is pushing the water out of the estuary. Figure 14 shows that new water represents 80% of the water inside the estuary at high water (lower part of the curve).

Analysis of the evolution of new water together with the location of tracers shows that water renewal is promoted mainly by tidal flow. This conclusion is consistent with the

---

<sup>2</sup> The simulation was done considering 10 thousand tracers. In areas where the contribution of new water is small, their density is high and graphical representation enhances the colour of tracers emitted by higher number origin (they are represented sequentially).

ratio between river discharge and tidal prism described above. Colour distribution in Figure 13 (having in mind footnote 2) shows high water mixing from different parts of the estuary, reinforcing the conclusion on the influence of water renewal.

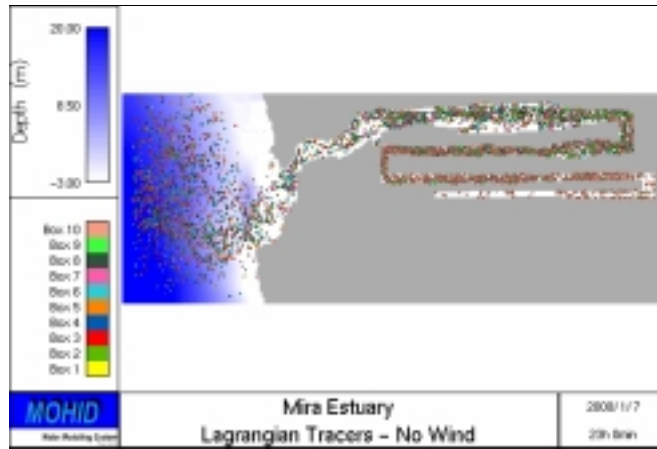


**Figure 12: Distribution of Lagrangian tracers in the Mira estuary after 7 days (No Wind).**

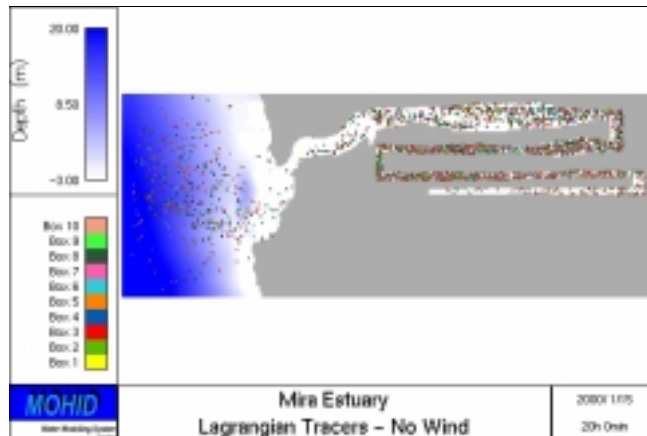


**Figure 13: Distribution of Lagrangian tracers in the Mira estuary after 15 days (No Wind).**

Figure 14 shows that 1 week after tracers releasing only about 40% of the initial volume remains inside the estuary and that after 2 weeks only 20% remain there. Defining the residence time as the time required for 80% of water to leave estuary, one concludes that, considering the most frequent river discharge and in the absence of a littoral current, residence time in the estuary is of the order of 2 weeks.

In case of littoral currents (generated by wind and ocean density), tracers leaving the estuary during ebb would have a smaller probability of re-entering during flood and

residence time would be smaller. Increasing river discharges would also decrease residence time. One can thus say that 2 weeks is a major residence time in the estuary.

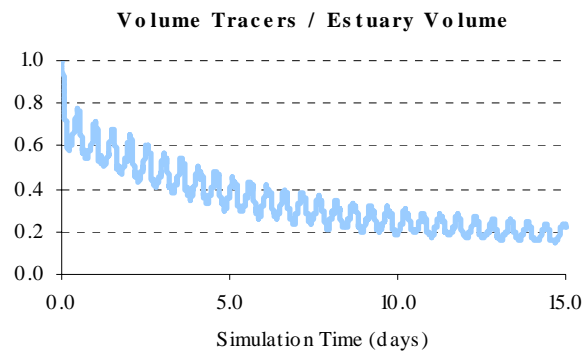


**Figure 14: Evolution of the ratio between the volume of lagrangian tracers inside the estuary and total estuary volume as a function of time (No Wind).**

### **3.5 INTERACTION BETWEEN PARTS OF THE ESTUARY**

The definition of residence time given in the previous paragraph accounts for time required for renewing a fraction of estuarine water, but does not account for the history of renewal processes. Interesting information to understand the properties of each region of the estuary is the interaction between that region and other regions of the estuary. This is particularly interesting in wide estuaries, but it is also interesting to know how fast the replacement of water in each part of the estuary is.

The same tool used for quantifying residence time in the estuary, can track the path of individual water masses. This tracking allows for calculating residence time in each box and for analysing the influence of each region of the estuary on the others. This information is presented in Figure 15 and Figure 16 in the form of “pie charts”. Slices are labelled according to the origin of water, being new water represented on white.

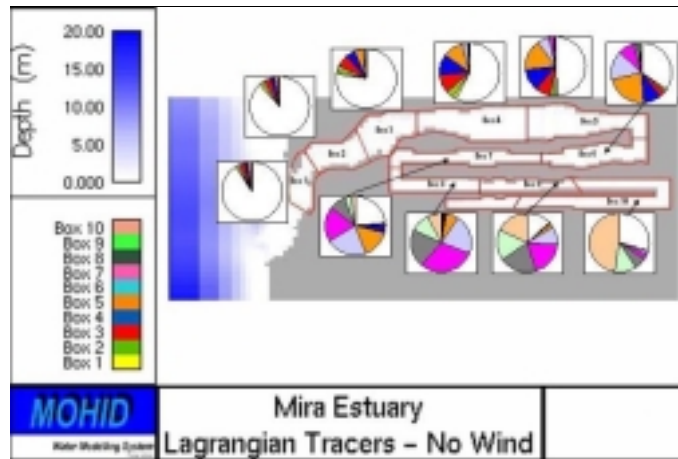


Figure 15: Water exchanges among boxes (results integrated period for 7 days).

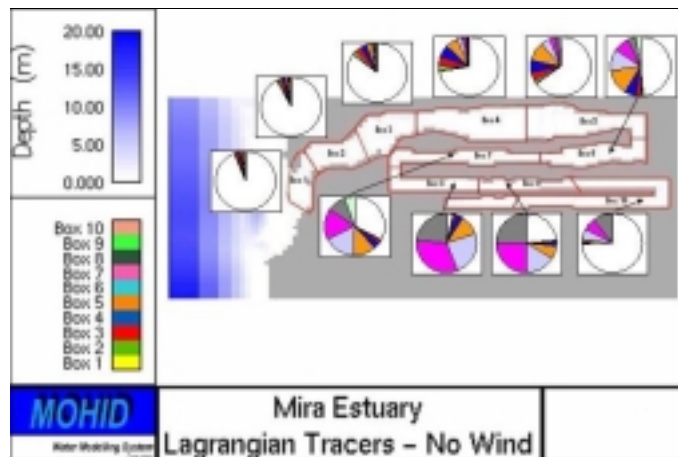


Figure 16: Water exchanges among boxes (results integrated period for 15 days).

Results were obtained integrating in time the composition of water inside a box and referring it to the total volume of water that was in the box. Figure 15 shows that in a period of 7 days, the water initially contained in box #10 contributes for about 50% of the properties of the box, while new water<sup>3</sup> (from the river) contributes with about 30%. By the contrary, in box #1, during the first 7 days about 90% of water in the box was new water. Comparing the inner boxes one can see that the contribution of marine water for the properties of the water inside each box decreases as one moves upward in the

<sup>3</sup> New water is in fact fresh water flowing from the river or marine water flowing from the open sea.

estuary, reaching only box #7 during the first week. The water from the river in one week reaches only two boxes (#9 and # 10).

Having in mind that the simulation started at high water, one can state that the upward progress of marine water is due to diffusion, since residual advection induced by the river is downward. Because river fresh water has progressed much less than marine water, one can conclude that longitudinal dispersion is the most effective transport process.

Figure 16 represents information identical to Figure 15, but for 15 days of integration. Comparison of both figures puts into evidence the estuary mixing with the extension of the influence of water released in the upper estuary downwards and of seawater influencing further upwards. The water originally in box #10, is already influencing box #7, while after one week it had only influencing box #9.

## 4 Ecological Model

The ecological model supports the understanding and quantification of ecological processes in the estuary and their dependency on loads and physical processes. Simulations were carried out for present conditions - reference situation – and for a scenario of nutrient load increasing. Results for the reference situation allow for model validation and the scenario of load increasing permits to evaluate sensibility and vulnerability of the estuary<sup>4</sup>.

### 4.1 REFERENCE SITUATION

Next paragraphs describe (i) field data used for imposing boundary conditions and for model validation, (ii) results of the model and their comparison with field data (model validation) and (iii) space and time integration analysis of results in order to obtain a global view of the ecological functioning of the estuary.

---

<sup>4</sup> A scenario of load increasing was preferred to a scenario of load reduction because the primary production in the estuary is limited by nutrients and is not realistic to assume that nutrients load can be reduced.

#### 4.1.1 Time Series Analysis (Field Data and Model Results)

This section describes model results and their comparison with field data. The field data available to validate the model results is scattered in time and space. Most relevant data on phytoplankton and nutrients was gathered by IPIMAR from February to October 1989 and by Silva de Almeida between December 1990 and October 1992.

The results of the model were integrated in boxes in order to simplify their comparison with field data. Figure 17 shows the location of IPIMAR stations (about 2 km apart) and the boxes used for integrating the results of the model. Silva de Almeida carried out measurements of nutrients in box #5 in the framework of a study of processes in a salt marsh. Table 2 shows IPIMAR and Silva de Almeida sampling periods.

**Table 2: Sampling periods in the Mira estuary.**

Station	Date	Reference	Parameters
#1, #3,#5,#7,#9	3/89 to 10/89	IPIMAR	Chl a
#5	12/90 to 10/92	Silva de Almeida	Nitrate, Ammonia

IPIMAR has published the spatial average values of Chl a (integrated in all stations) for each month from March to October of 1989 for high and low water and the time averaged values of Chl a for each station during the sampling period. Figure 18 compares the time series published by IPIMAR with the time series of the average of all boxes computed by the model. Field data are represented by yellow (high water) and red (low water) dots and model results by blue dots. Comparison shows a very good agreement, except for two low water dots in April and July. These two measurements seem to be anomalous. In fact, in the same day, high water values show the same trend has in other months, suggesting that samples were collected in water masses with very specific properties, not representative of the estuary.





**Figure 17: Location of field Stations of IPIMAR’s campaigns and correspondent box for each station in Mira estuary.**

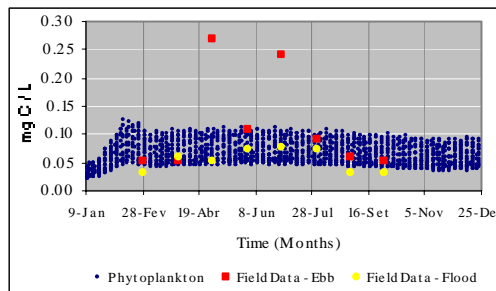


**Figure 18: Time series of model results (blue points) for whole estuary and phytoplankton field data for 1989 (IPIMAR) in the reference situation.**

Figure 19 compares for each station annual high water and low water average values of phytoplankton, ammonia and nitrate with average values computed by the model in the corresponding integration boxes. In the lower estuary, where marine influence is higher, the model and data show very similar results. In the upper estuary, results of the model<sup>5</sup>

---

<sup>5</sup> Results of the model are integrated in time, because their splitting into high water and low water would require extra software development.

merge quite well with field data only at low water. This is due to an overestimation of dry season river discharge in the model.

The consideration of a time variable river discharge would require much more computing time and was not considered. This discrepancy between simulated and measure values are not a problem for the purpose of this study. The goal is to assess eutrophication in the estuary and considering a river load higher than the real one, can be seen as a safer scenario.

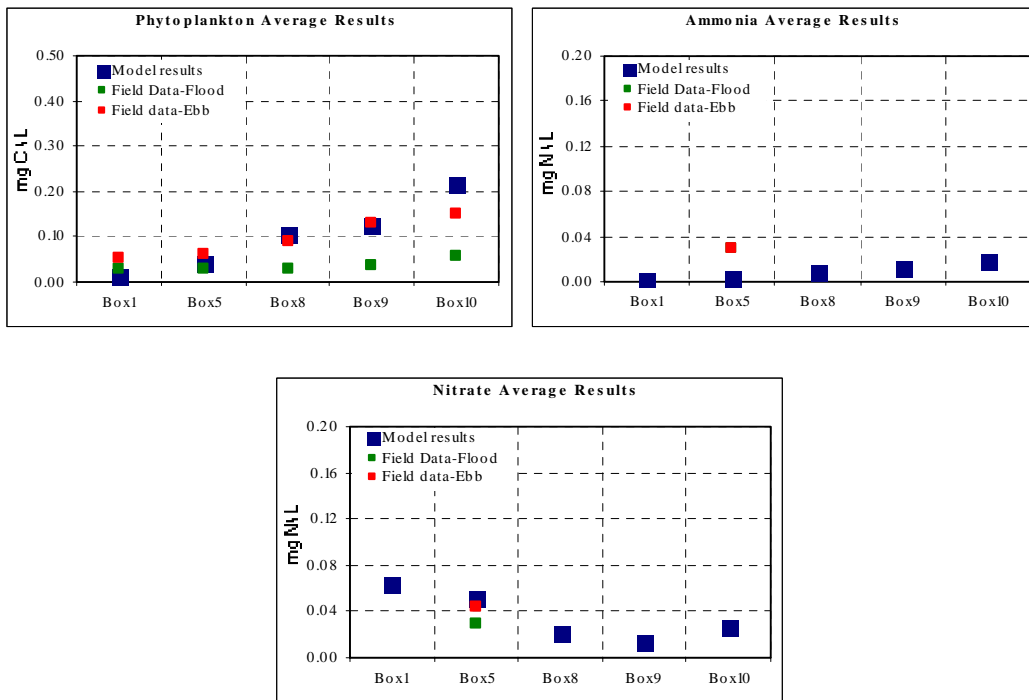


**Figure 19: Annual average concentrations computed by model and measured in boxes for reference situation.**

Combining model results and field data allows gaps filling, making possible the analysis of the estuary behaviour. Results show that nutrients concentration and phytoplankton are quite low in the whole estuary and that their value decreases as one moves towards the mouth. Figure 20 to Figure 24 represent time series of model results. The figures show daily and seasonal evolution of concentration of phytoplankton, nitrate, nitrite and dissolved oxygen.

The figures show that tidal variability tends to be more important than seasonal variability. This is also suggested by field data presented in Figure 18 (except for the two anomalous points in April and July, commented before). The figures also show that

the lower estuary imports nitrate from the sea. The value at high water is equal to the value off the mouth, which tend to be quite uniform during the whole year due to coastal mixing processes.

Nutrient concentrations tend to be very small. They decrease downstream from the river boundary, to reach a minimum in the middle of the estuary and then it increases again towards the ocean boundary. This behaviour put into evidence the biological consumption and nutrients limitation. In the middle estuary phytoplankton also decreases due to grazing. In the upper estuary, at the beginning of February there is a tendency for generation of a bloom, which has no time to develop due to nutrient limitation. In the lower estuary, nitrate increase due to ocean water input, but the local residence time is not large enough for phytoplankton to grow.

#### **4.1.2 Spatial Distributions of Concentration**

Spatial distributions of phytoplankton, ammonia, nitrate and oxygen are presented in Figure 25. The figures show the upstream and downstream zone of estuary. It is possible to verify that concentrations are higher during ebb than flood, because during ebb the volumes of water in the estuary diminish.

The figures also show that most intense biological activity occurs at the upper part of the estuary mostly because of nutrient availability from river discharge. The dilution effect in the downstream direction, that was already mentioned, is quite visible in all results, especially the effect on nitrate increase near the mouth caused by nitrate rich ocean waters. River discharge is the most relevant source of ammonia and nitrate. These figures are useful for a quick overview of the estuarine conditions, but are not enough to characterize the role of each area for the whole estuary. In the next paragraphs a description of the exchanges between boxes will be presented. Comparison between scenarios will be based on the results integrated inside each box.

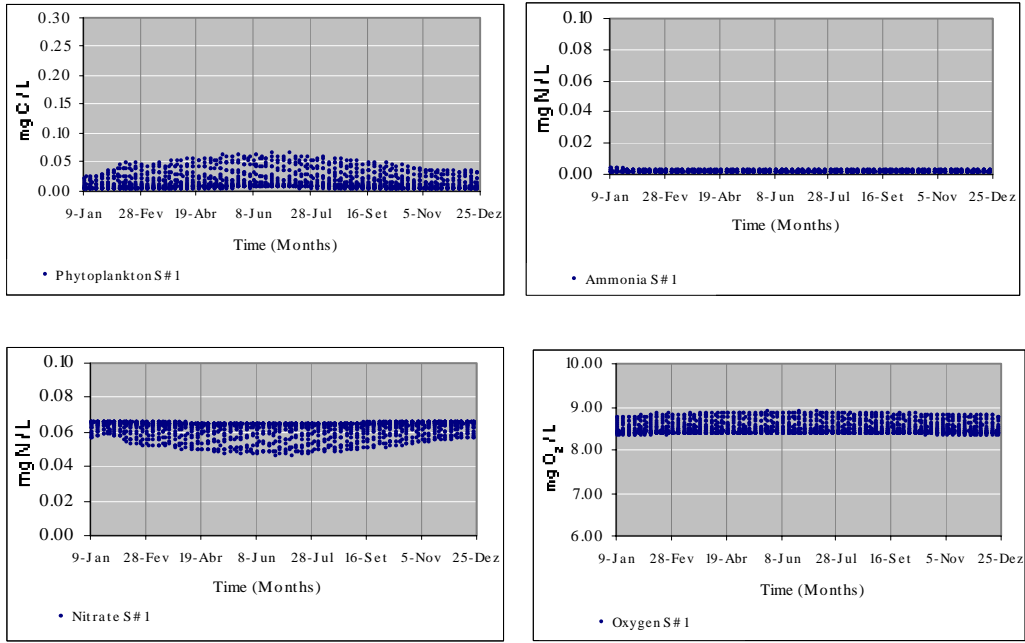


**Figure 20: Time series of model results in Station#1 for reference situation.**

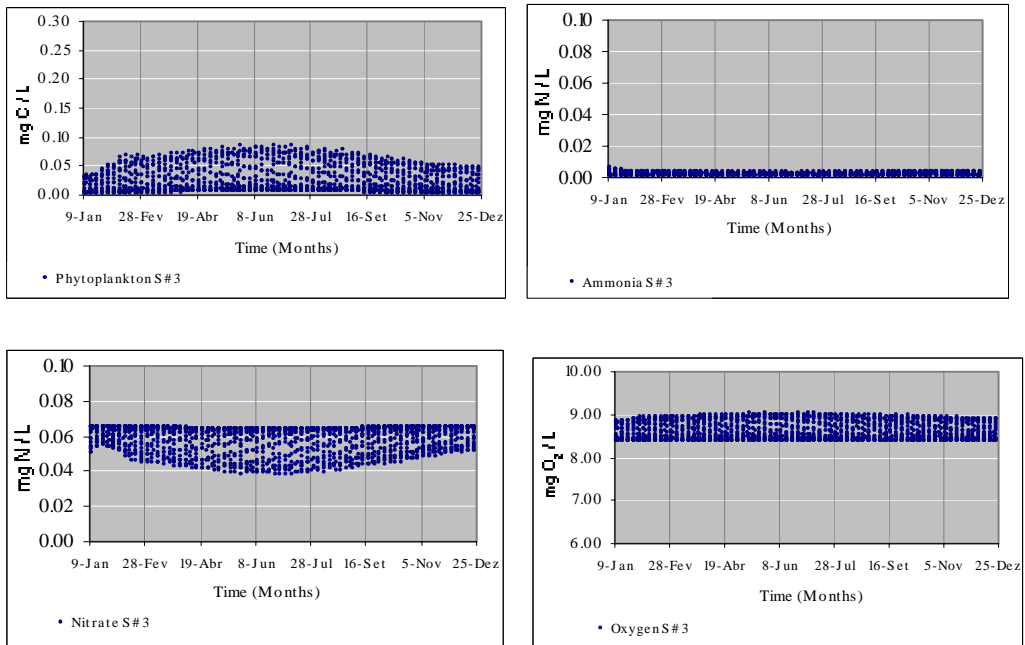


**Figure 21: Time series of model results in Station#3 for reference situation.**

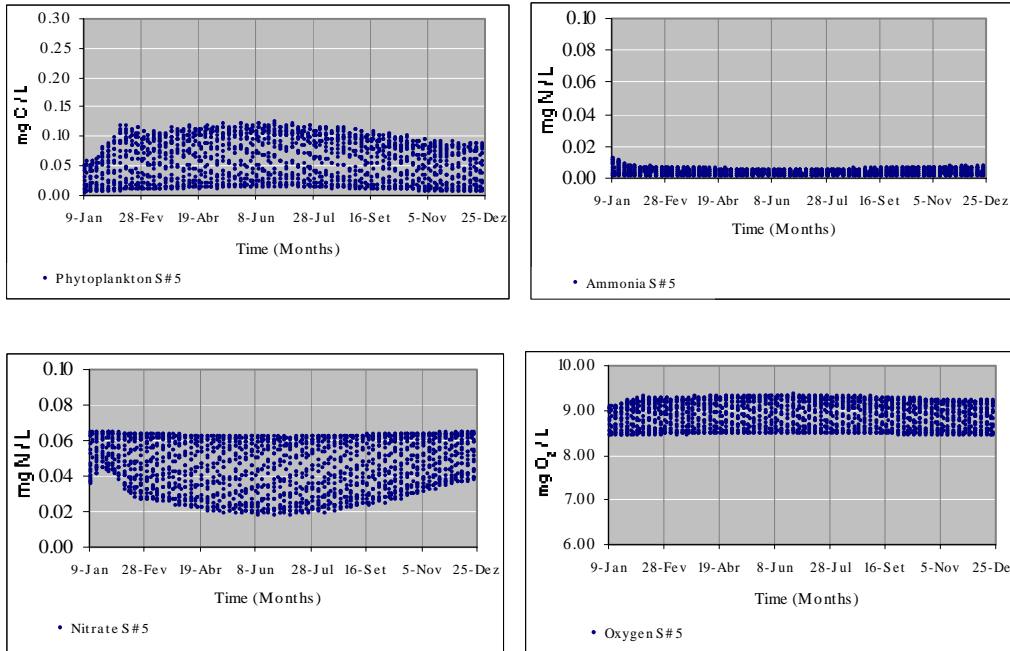


Figure 22: Time series of model results in Station#5 for reference situation.

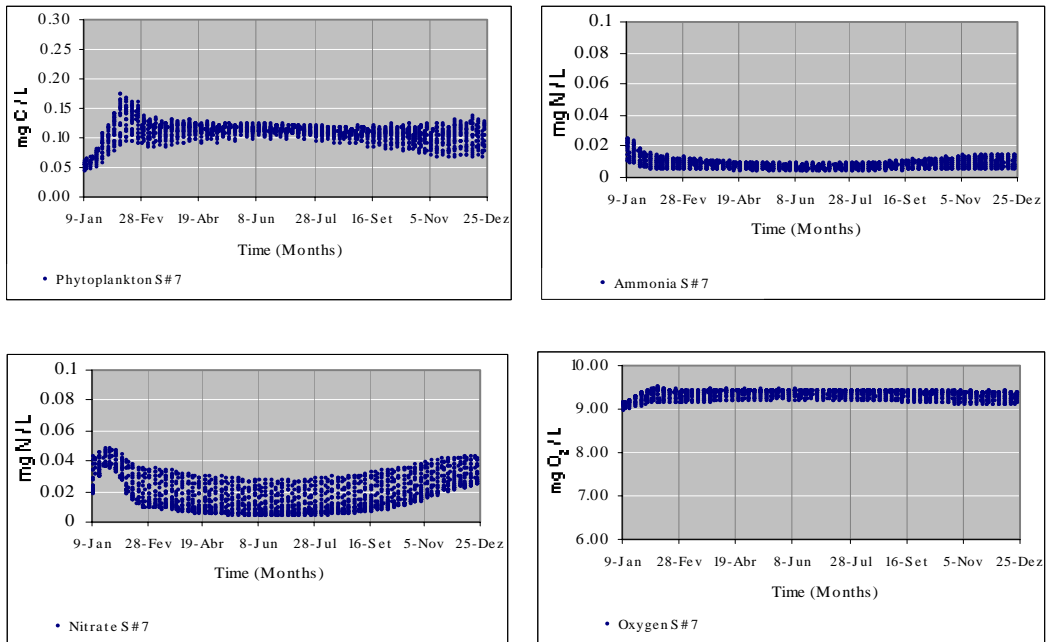


Figure 23: Time series of model results in Station#7 for reference situation.

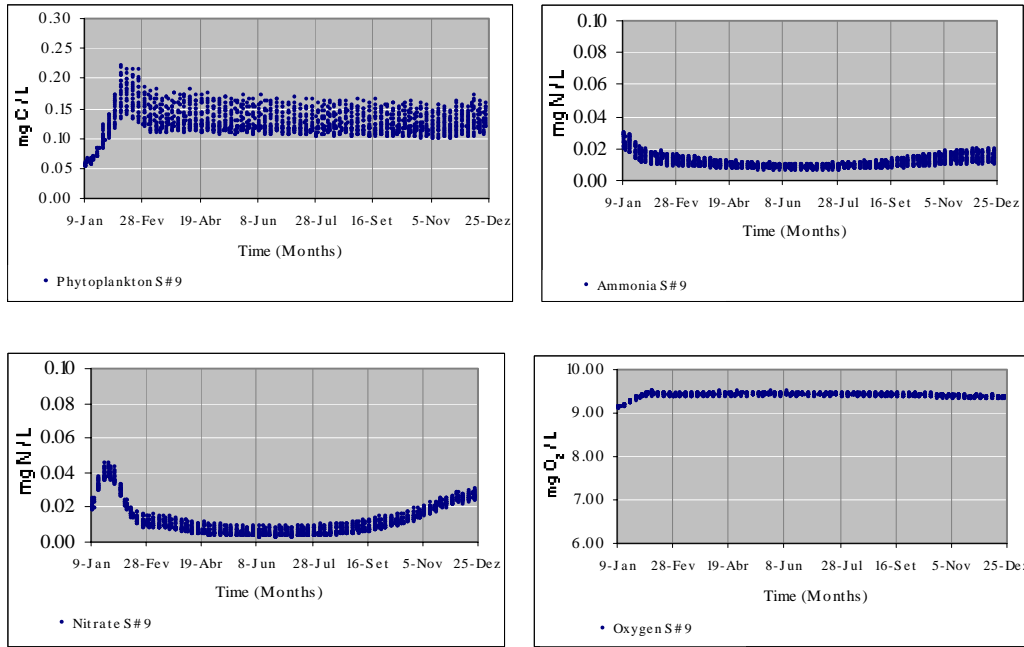


Figure 24: Time series of model results in Station#9 for reference situation.

#### 4.1.3 Annual Average Distributions of Properties per Zone of the Estuary

Average values of phytoplankton, ammonia, nitrate and organic matter per box and net fluxes between boxes are shown in Figure 26. Organic matter is defined as a sum of PON (Particulate Organic Nitrogen) and DON (Dissolved Organic Nitrogen) in the water column. This figure shows, clearly, that the concentrations tend to diminish towards the ocean, while nitrate tends to increase. This is due to mixing of estuarine and marine waters. Maximum values of phytoplankton, ammonia and organic matter occur in the upper estuary.

Figure 27 shows cumulative frequencies of phytoplankton in the upper estuary, in the mixing zone and in the lower estuary. This figure shows that 100% of phytoplankton values are below 5  $\mu\text{g Chl a/L}$  in the marine zone, while in the mixing zone and in the fresh zone of the estuary, 94% of the computed values are below that value.

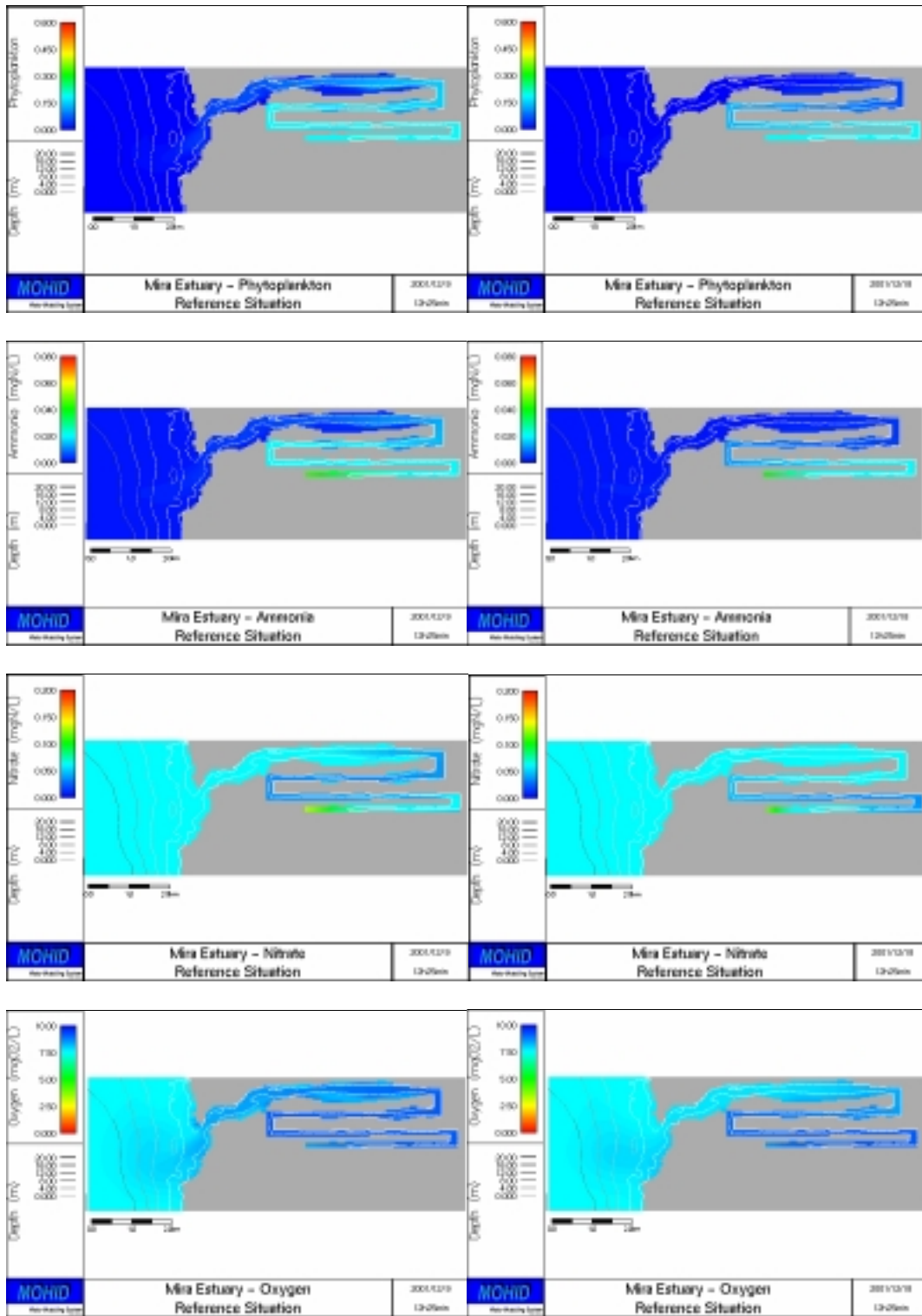


Figure 25: Spatial distribution of phytoplankton, ammonia, nitrate and oxygen in the reference situation during ebb (left) and flood (right).

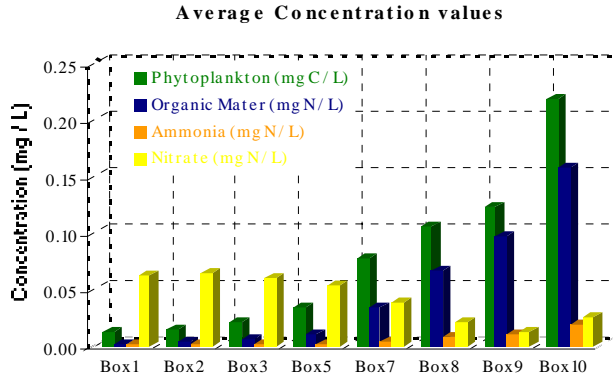


Figure 26: Annual average values of Phytoplankton, OM, Nitrate and Ammonia per box in the estuary for the reference situation.

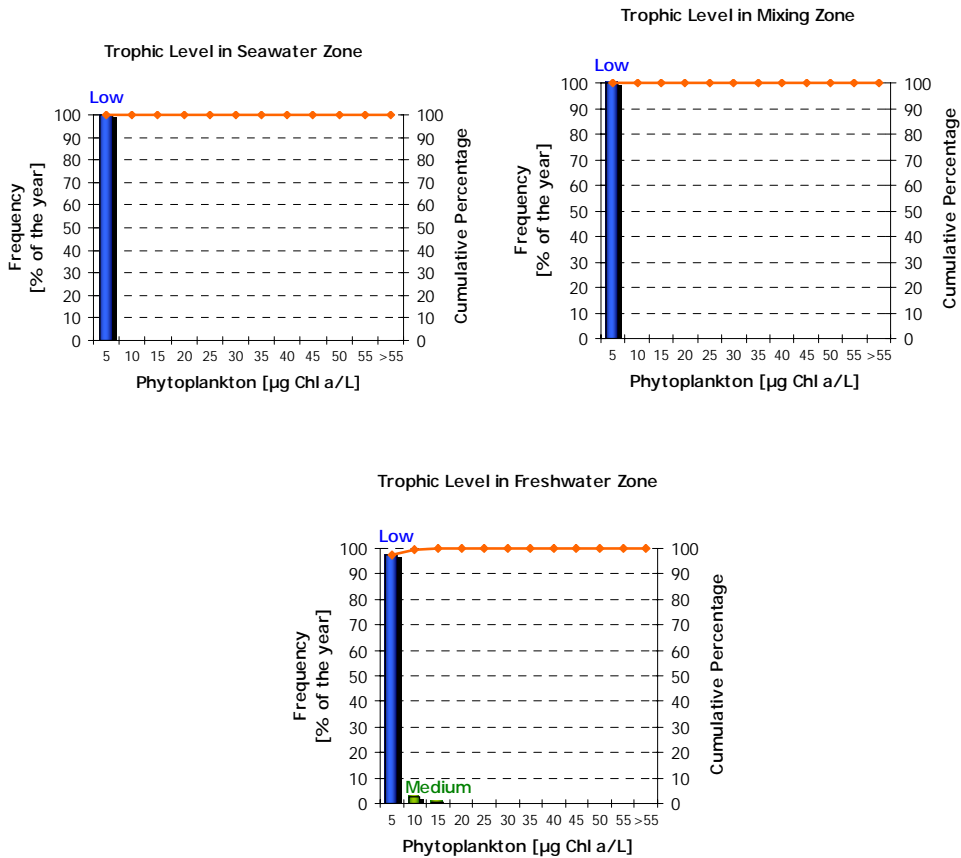


Figure 27: Cumulative frequency for phytoplankton in Seawater, mixing and freshwater zones.



According to the classification proposed by the-NEEA applied to Mira estuary<sup>6</sup> the estuary can be classified as a *low* trofic activity estuary on the basis of the cumulative frequencies shown in Figure 27.

#### **4.1.3.1 Annual Budgets per Zone of the Estuary**

Figure 28 represents the annual net exchanges between boxes (ton/year) of phytoplankton, ammonia, nitrate, organic matter and zooplankton. The same information is shown in Figure 29 on spatial basis. Global budgets for the whole estuary are represented in Figure 30. The figures show that the estuary is a net exporter of phytoplankton, zooplankton and organic matter and imports nitrate. In case of ammonia, the annual budget is balanced showing that production by biological activity (OM mineralization and excretions) is balanced by consumption. The estuary imports marine nitrate because consumption in the middle estuary reduces its concentration to levels below concentration in the sea.

#### **4.1.3.2 Conclusion of reference situation**

Phytoplankton is clearly bottom limited by nutrients availability, but also top limited by zooplankton grazing. Low residence time reduces oxygen consumption in mineralization processes, making the estuary a net exporter of organic matter. Nitrate depletion inside the estuary generates a net flux of nitrate from the ocean into the estuary. Based on the results of model, the estuary would be classified as *low* trofic level accordingly to the NEEA index, as it was on the bases of the available field data.

---

<sup>6</sup> Identification of Sensitive and Vulnerable Zones in 4 Portuguese Estuaries. Application of the United States National Estuarine Eutrophication Assessment to the Mira, Mondego, Sado and Tagus Estuaries. J.G. Ferreira, T. Simas, K.Schifferegger and J. Lencart Silva. INAG, 2002.

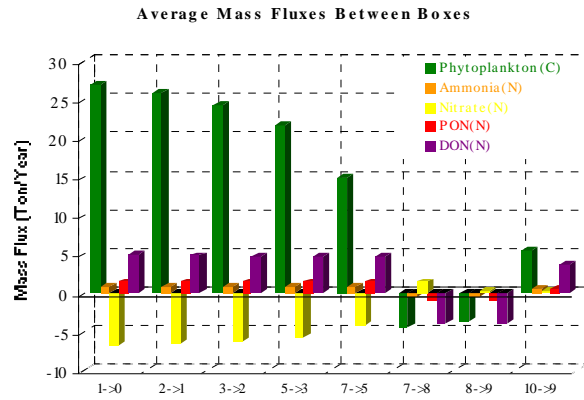


**Figure 28: Annual Mass Fluxes between zones of Estuary.**



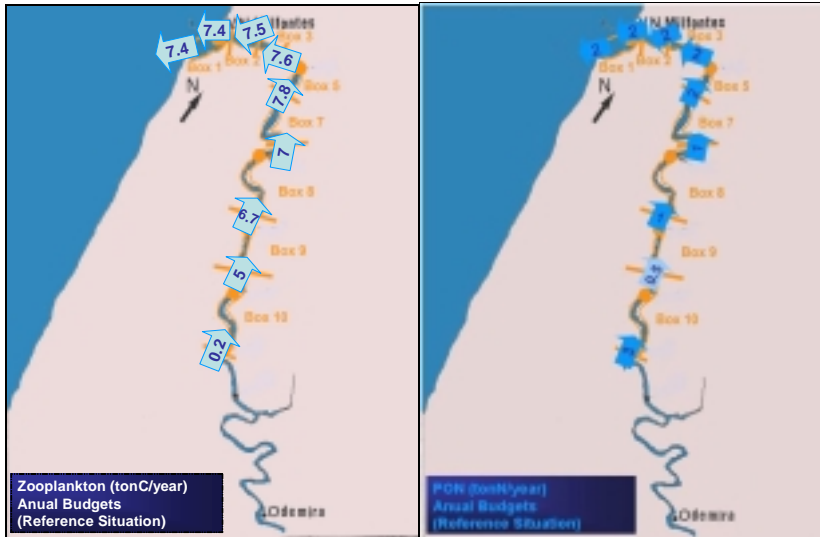


Figure 29: Annual budgets between boxes in the reference situation.

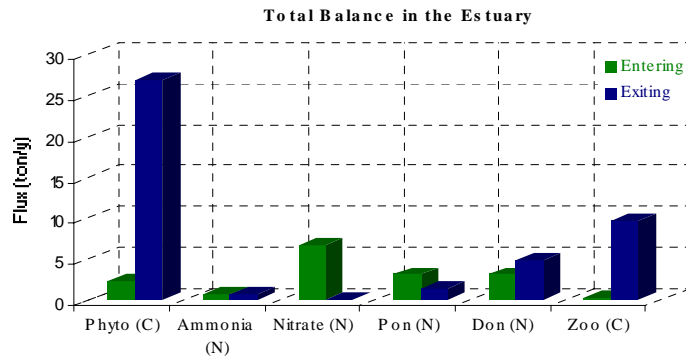


Figure 30: Total Balance in Mira Estuary for Reference Situation.

#### 4.1.4 Scenario of Nitrate Discharge Increasing

In order to support decision-making in terms of nutrients management a scenario of nutrients variation was tested. If concentration of nutrients were high in the estuary, a reduction scenario would be the most adequate. In Mira estuary conditions, where nutrients are the most important limiting factor, a nutrient-increasing scenario is more interesting. A duplication scenario was chosen. All parameter values are the same used in the reference situation simulations.

#### **4.1.4.1 Spatial Distributions**

Figure 31 compares spatial distributions for the reference situation (left) and for a scenario of nutrient load duplication (right), considering winter conditions, when biological activity is lower and nitrate is less limitative. This figure shows that a duplication of nutrients in Mira River induces only a very slight increase in nitrate concentration close to the river boundary, and has a negligible influence on the concentration of the other represented variables. In the mixing zone, even during winter, concentration of nitrate is still below concentration in the sea and consequently, even in winter, the estuary remains a net importer of nitrate.

Analysis of the results along the whole year shows that phytoplankton productivity increases as a consequence of nutrient load increase, but production is consumed by zooplankton. This result shows that in the Mira phytoplankton is bottom limited by nutrients and top limited by zooplankton. As a consequence an increase of nutrients increases the biomass of secondary producers and not the concentration of phytoplankton.

#### **4.1.4.2 Annual Distribution**

Figure 32 represents the differences between reference situation and nitrate increasing scenario. In all boxes, nitrate concentrations are higher in the scenario with an increase nitrate river load, as was expected. Ammonia and organic matter concentrations increase slightly in all boxes as consequence of an increased biological activity. For phytoplankton an interesting situation occurs. The upstream boxes (boxes 10, 9) show a phytoplankton increase, while between box 8 and box 3 phytoplankton slightly decreases in double nitrate load scenario. In the boxes closer to the ocean, concentration is the same for both scenarios. Secondary productions explain these results.

On upper boxes phytoplankton grows more intensely in nutrients increasing scenario and is advected downstream. The length of the zone where phytoplankton increases is related with time required for zooplankton to grow and downstream advection. In the middle estuary population of zooplankton is already large enough to decrease concentration of phytoplankton below its concentration in reference situation. In the lower estuary concentration is strongly influenced by ocean conditions and no differences are registered between scenarios.

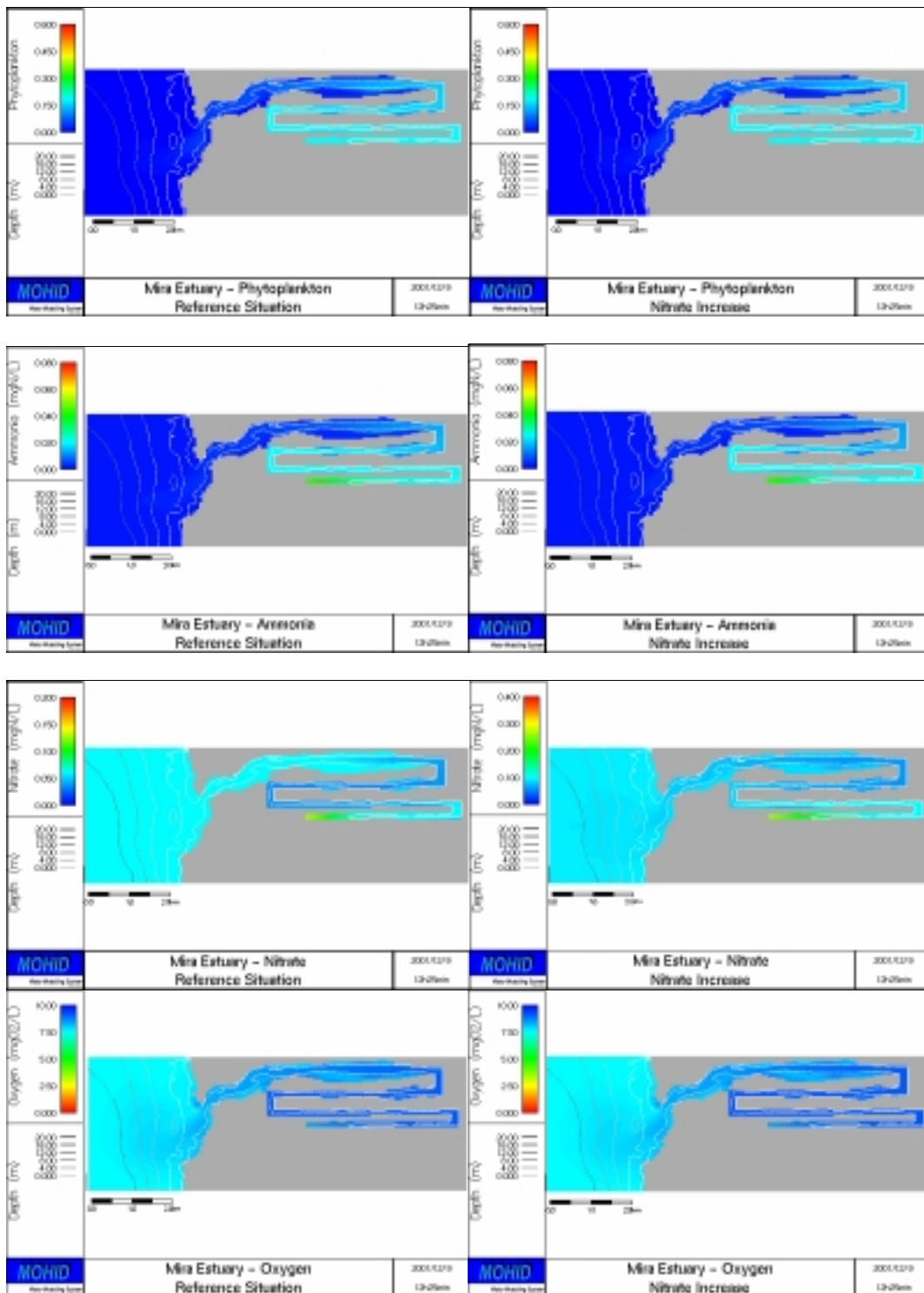
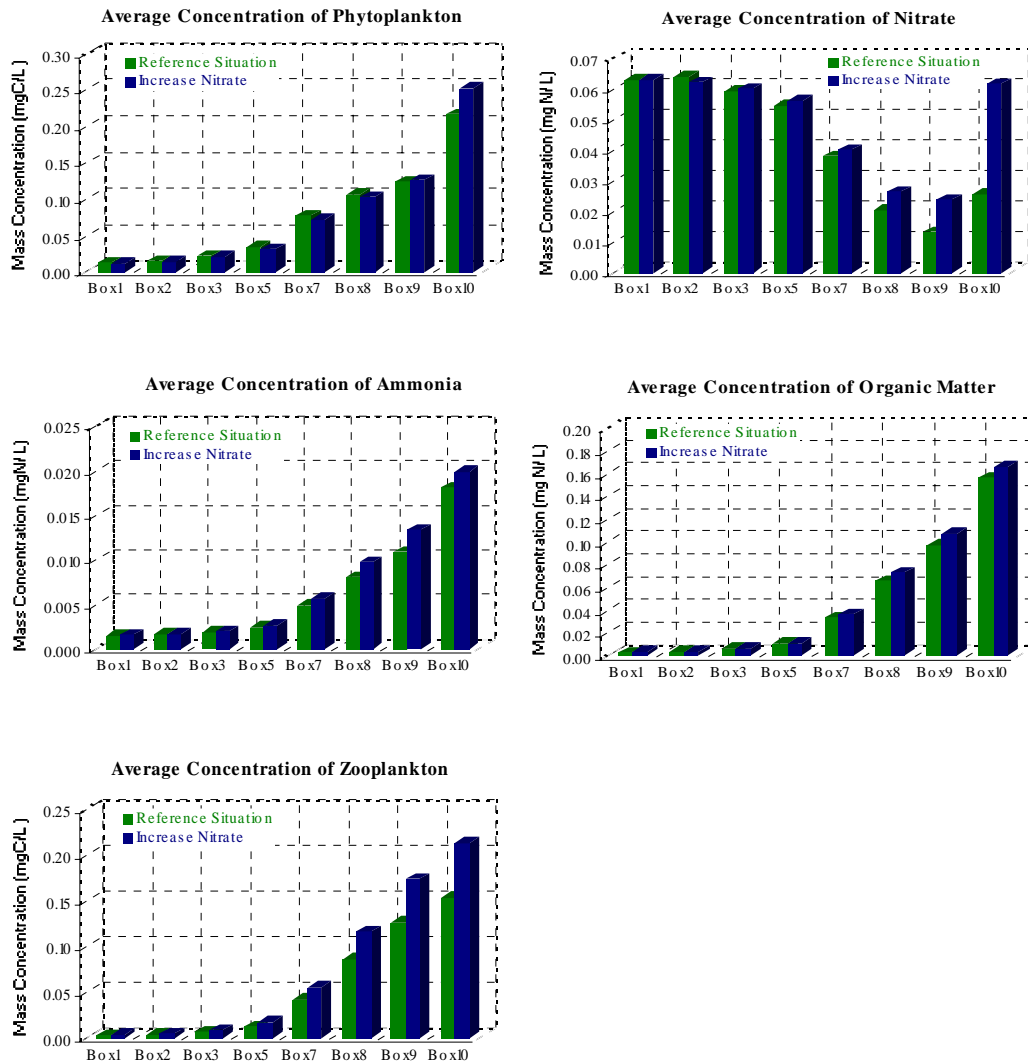


Figure 31: Comparison of concentrations for reference situation (left) and a scenario of nitrate load doubling (right) (winter, low water scenario).



**Figure 32: Average Annual concentration in reference situation and in double nitrate river load scenario.**

Figure 33 shows oxygen required for oxidation of organic matter in each box for both scenarios, and shows that oxygen consumption is higher in nitrate increase scenario, since there is a larger production of organic matter.

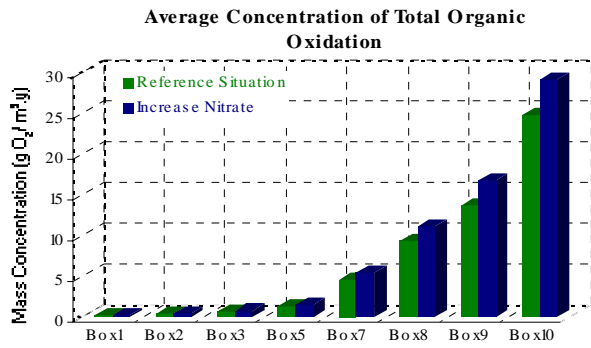
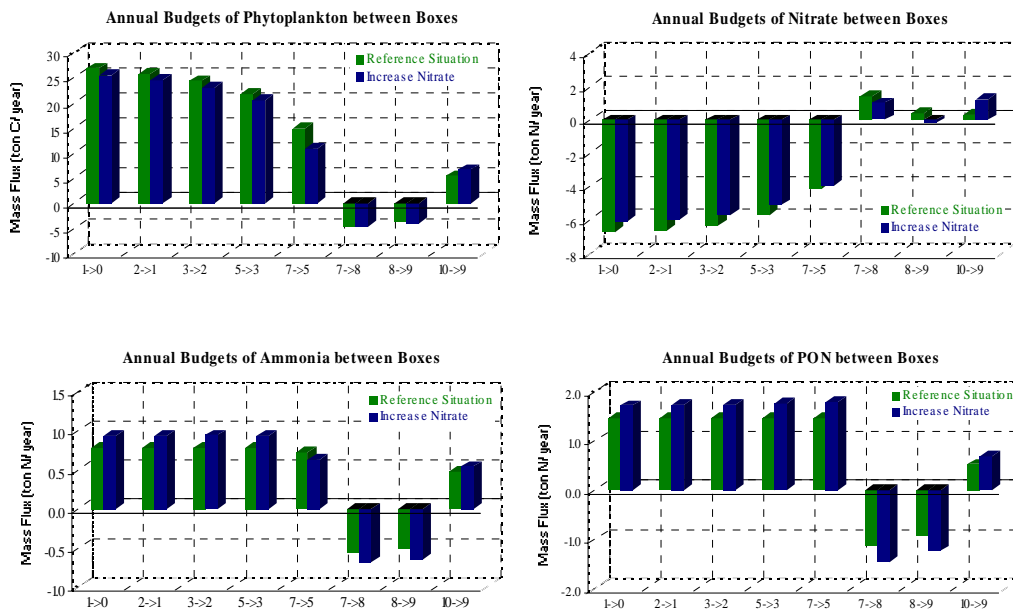
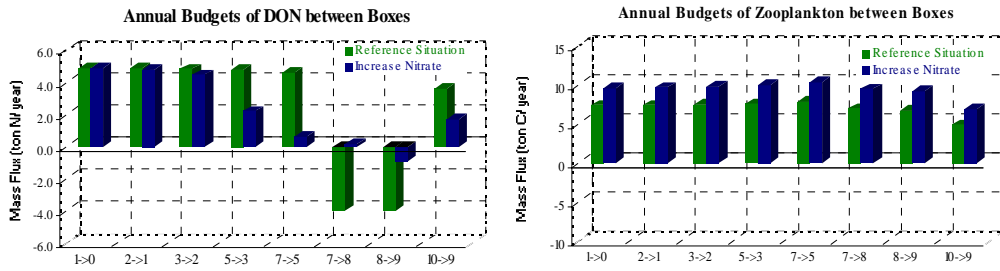


Figure 33: Oxygen consumption for oxidation of Organic Mater in reference situation and in double nitrate river load scenario.

#### 4.1.4.3 Annual Budgets per Zone of the Estuary

The main consequence of nitrate load increase is a decrease of nitrate imported from the ocean and an increase in the export flux of organic matter and ammonia. The phytoplankton export flux also decreases slightly but mostly because there is an increase in zooplankton export flux so globally the carbon flux from the estuary to the ocean increases.





**Figure 34: Annual Budgets in the reference situation and in the scenario of doubling nitrate river load.**

Figure 35 shows the total balance of the most important properties for the whole estuary, for both scenarios. Figure confirms previous conclusions.

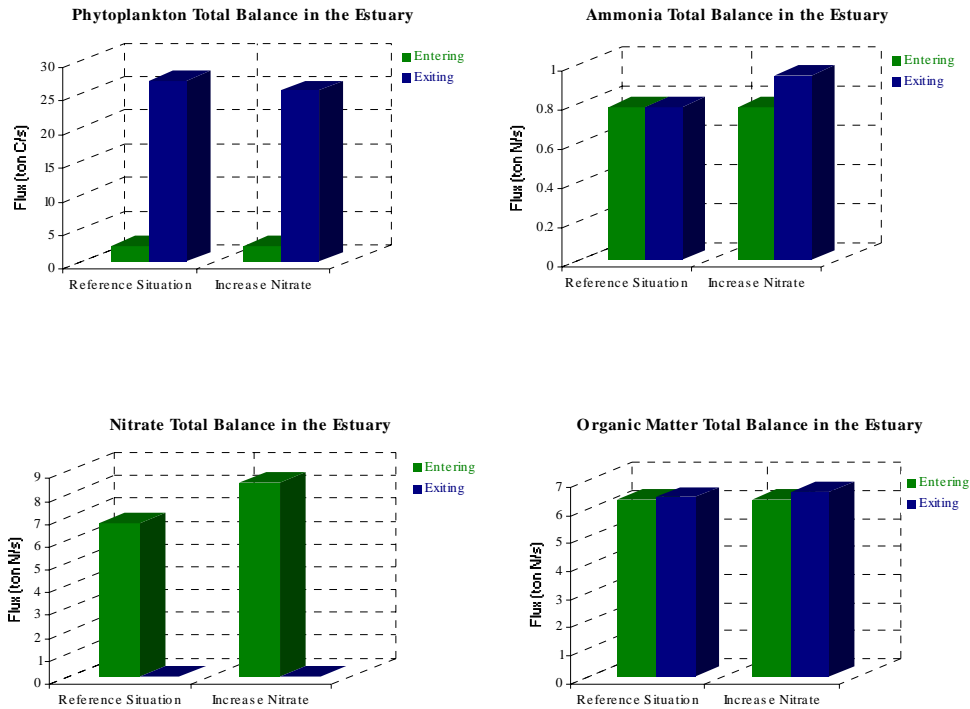


**Figure 35: Total Balance of estuary in the reference situation and in the scenario of doubling nitrate river load.**



## 5 Conclusions

Trophic processes in the Mira were studied using an eco-hydrodynamic model in a reference situation and in a scenario of doubling nitrate river load. Hydrodynamics is forced by tide and by river discharge. The model is vertically integrated and uses a grid size varying from 20 meters close to the mouth, until 200 meters in the upper estuary. An oceanic buffer zone off the estuary was considered to allow processes simulation in the ebb water that re-enters the estuary during flood.

Residence time was computed using the movement of lagrangian tracers. The same tracers were used to study the interdependency between different regions of the estuary and to visualise the water refreshing process in the estuary. Results show that residence time in the estuary in low river discharge conditions ( $0.5 \text{ m}^3/\text{s}$ ) is of the order of 2 weeks and that time required for water refreshing in the lower estuary is of the order of days. Results also show that longitudinal dispersion connected to tidal oscillation is the main mechanism determining residence time in the estuary. Advective flow associated to the most frequent river discharge has a secondary order contribution for residence time.

Trophic processes in the estuary are directly linked to its physics. The quantity of nutrients discharged by the river is not enough to maintain trophic activity in the estuary, which becomes a net importer of nitrate from the sea. Nutrients are transported by diffusion processes associated to the tidal flow and are consumed in the middle estuary where their concentration decreases much below concentration in the sea. Phytoplankton and organic matter (dissolved and particulate) produced in this region of the estuary is added to that produced upstream using nutrients discharged by the river and are exported to the sea.

Results show that trophic activity in the estuary is bottom limited by nutrient availability and top limited by secondary production. The estuary is a net importer of nitrate and exports phytoplankton, organic matter and zooplankton. The export of organic matter is a consequence of the low residence time in the lower estuary, which promotes exportation of organic matter before mineralization, reducing the consumption of oxygen inside the estuary. Top control by zooplankton was enhanced in the simulation of nutrient increase scenario.

As a consequence of nutrient limitation and of predation of zooplankton, concentration of phytoplankton is below 5  $\mu\text{g/L}$  in whole the estuary during most of the year. Concentrations above 5  $\mu\text{g/L}$  were obtained only in the upper estuary, but for less than 5% of the time. Based on these results the estuary should also be classified as a *low* trophic level, according to the index proposed by the NEEA and applied to Mira estuary by Ferreira *et al*, considering field data, and also classified as *low*.

## Annex - Waste Water Treatment Plants

Odemira and Vila Nova de Milfontes are two most important agglomerations in the vicinity of Mira estuary located respectively immediately upstream of the estuary and at the mouth. This annex provides information on the loads from these stations, having in mind the population equivalent and measurements in the influent and effluent of the stations. Odemira City Council provided monitoring data and data about the number of inhabitants.

Table 3 gives the location, size and type of treatment for each station, showing that both stations are quite small.

Table 4 shows the loads estimated for each station considering average values per inhabitant and the Population Equivalent served by each WWTP and typical efficiencies for each kind of treatment. The parameters used to obtain data listed in

Table 4 starting from data listed in Table 3 are listed in Table 5 and Table 6.

Odemira WWTP discharges at the River, upstream from the limit of the estuary and its load as been added to river discharge. Vila Nova de Milfontes discharges directly into the sea and hasn't been considered since the load is smaller than the uncertainty of the open ocean boundary condition.

**Table 3: Odemira and V. N. de Milfontes Waste Water Treatment Plant characteristics.**

Name	Portuguese Co-ordinates		Geographical Co-ordinates		Population Equivalent	Situation	Treatment Type
	M	P	Latitude	Longitude			
Odemira	61700	230330	37° 35' N	8° 49' W	2200	Working	Secondary
Milfontes	58400	215000	37° 43' N	8° 47' W	3000	Working	Primary

**Table 4: Loads estimated before and after each treatment plant.**

WWTP Name		Flow (m <sup>3</sup> /s)	Total Solids (mg / L)	BOD (mg O <sub>2</sub> / L)	Nitrate (mgN/L)	Nitrite (mgN/L)	Ammonia (mgN /L)	DON Refractory (mg N /L)	DON Non Refractory (mg N /L)	PON (mg N /L)
Odemira	Before	0,003	755.8	500	15	10	26,7	11,4	26,5	37,9
	After	0,003	113.4	50	15	10	24,0	9,4	0	32,2
Milfontes	Before	0,007	453.5	300	15	10	16,0	6,8	15,9	22,8
	After	0,007	226.8	240	15	10	16,0	4,8	11,1	13,7

**Table 5: Typical values of loads per inhabitant per day (Saraiva, 2001).**

Properties		Typical Value
Flow		200 L /inhabitant/day
Total Solids		90,7 g / inhabitant/day
Biochemical Oxygen Demand (CBO <sub>5</sub> )		60 g / inhabitant/day
Inorganic Nitrogen	Nitrite	10 mg N / L
	Nitrate	15 mg N / L
	Ammonia	3,2 g N / inhabitant/day
Organic Nitrogen	Total	9,1 g N / inhabitant/day
	Dissolved Non Refractory	35%
	Dissolved Refractory	15%
	Particulated	50%

Values of nitrite and nitrate are independent of the number of inhabitants because domestic use of water doesn't change much those properties. The values indicated are majors of current values in supplying water<sup>7</sup>.

**Table 6: Removal Efficiency of WWTP considered when no measured data was available (Saraiva, 2001).**

Property		Primary Treatment	Secondary Treatment	Secondary Treatment with Denitrification
Total Solids		50%	85%	85%
Biochemical Oxygen Demand (BOD <sub>5</sub> )		20%	90%	90%
Inorganic Nitrogen	Nitrite	0%	100%	100%
	Nitrate	0%	0%	85%
	Ammonia	0%	10%	10%
Dissolved Organic Nitrogen	Total	10%	30%	30%
	Refractory	3%	15%	15%
	Non Refractory	3%	100%	100%
	Particulate	4%	15%	15%

<sup>7</sup> Values measured in the Mira River and shown in Figure 3 display concentrations of the order of 0.2 mg/L.